Penetration of *n*-Hexadecane and Water into Wood under Conditions Simulating Catastrophic Floods

Ganna Baglayeva   Wayne S. Seames   Charles R. Frihart

Jane O'Dell   Evguenii I. Kozliak

Abstract

To simulate fuel oil spills occurring during catastrophic floods, short-term absorption of two chemicals, *n*-hexadecane (representative of semivolatile organic compounds in fuel oil) and water, into southern yellow pine was gravimetrically monitored as a function of time at ambient conditions. Different scenarios were run on the basis of (1) the order of contamination (*n*-hexadecane followed by water or vice versa) and (2) whether the wood lateral sides were covered with epoxy. The experiments were designed to evaluate fast initial sorption, allowing separate estimation of the end-grain (i.e., total longitudinal) and lateral (i.e., surface longitudinal) liquid penetration. Presaturation of wood with water did not significantly impede the subsequent penetration of *n*-hexadecane, whereas the presaturation of wood with *n*-hexadecane led to a significant decrease of the subsequent water uptake. This difference in penetration on the basis of the order of application was explained by the differences in the polarities of the two penetrating liquids and their impacts on the interactions with the wood matrix. Calculated apparent diffusivities for end-grain and lateral penetration were similar at ca. 3×10^{-7} m^2/s, indicating that filling of easily accessible near-surface voids does not have a substantial impact on the overall penetration of contaminants into wood. The *n*-hexadecane distribution profiles based on penetration into wood blocks (obtained by means of gas chromatography) showed that water and *n*-hexadecane appear to use different (although overlapping) penetration paths owing to the differences in their physical properties.

Semivolatile organic chemicals may be introduced into wooden structures by the spillage of petroleum-based liquids such as fuel oil, lubricating oils, and diesel fuel. Semivolatile organic chemicals may also be introduced into wooden members by design, e.g., as wood preservatives, or by modification such as by acetylation. A severe case is the contamination of wood during catastrophic floods due to the spill of fuel oil into flood waters, which then contacts wooden framing members and subflooring. Liquid hydrocarbons and water are virtually immiscible. Although water is soluble in hydrocarbons up to 1 mM at room temperature, the solubility of hydrocarbons in water drops significantly within the homology series, decreasing from 1 to 0.1 μM for *n*-hexane and octane, respectively, and then by two more orders of magnitude for *n*-hexadecane (Possani et al. 2014). Because many of the chemicals in fuel oil and other similar oils are only semivolatile (e.g., *n*-hexadecane has a boiling point of 287°C), they are difficult to remove by evaporation or leaching. As a result, they desorb at a very low rate over a long period of time, causing persistent odors.

A deep understanding of the nature of semivolatile organic chemical penetration through wood is necessary so that remediation methods can be developed. This article documents part of a comprehensive study conducted by the authors into this subject.

Wood's chemical structure consists of three main polymeric components: cellulose, hemicellulose, and lignin, of which cellulose and hemicellulose are primarily hydrophilic, whereas lignin is fairly hydrophobic (Siau 1995). The wood capillary microstructure (such as the geometry, type, and dimensions of the cells) has a major influence on the absorption of liquids. The porous heterogeneous structure of wood results in both strong adsorption (a surface process)

and strong absorption (a bulk process) of both polar and nonpolar chemicals, such as water and organic contaminants (Marcovich et al. 1999). Because of the complexity of the cell structure and the range of effective channel sizes and surface areas, we use the term ''sorption'' to refer to the combined process of solvent transport in wood.

Typical penetration channels in wood are longitudinal tracheids, interconnected by pits, resin canals (characteristic for southern pines [Siau 1995]), and wood rays (Comstock 1970). Polar chemicals can also penetrate through wood cell walls and side-grain cracks, resulting in wetting of the cellulosic portion of the wood, opening of blocked cells, and wood swelling (Forest Products Laboratory 1999). Along with longitudinal tracheids, other microscopic diffusion paths occur, although they are often blocked by tyloses, gummy deposits, and bordered pits (Stone and Forderrenther 1956). The presence of air in wood cell voids further limits the rate and amount of penetrating liquid (Malkov et al. 2001). Because of the occurrence of tracheids, the end-grain (longitudinal) sorption is two to three times greater than side-grain (transverse) sorption (Siau 1995). High absorption rates were also detected at the surface, i.e., in open-ended tracheids formed by sawing (Smith and Purslow 1960, Marcovich et al. 1999, Morgan and Purslow 1973).

The most versatile way to study initial (i.e., short-term) end-grain sorption of chemicals in wood is by either full immersion or dipping the wood samples into the liquids of interest (Smith and Purslow 1960; Morgan and Purslow 1973; Petty 1975, 1978a, 1978b; Chin et al. 1999; Kumaran 1999; Barrera-García et al. 2008; Khazaei 2008) and measuring the sample mass changes at pertinent time periods. To accurately represent the real-world contamination of building members, sorption experiments must be performed at ambient conditions. To date, only water (Comstock 1970, Chin et al. 1999, Koponen 1999, Kumaran 1999, Marcovich et al. 1999, Malkov et al. 2003, Khazaei 2008) and wood preservation agents dissolved in water (Stone and Forderrenther 1956, Smith and Purslow 1960, Petty 1978a, Krabbenhoft and Damkilde 2004, Barrera-García et al. 2008) have been studied as penetrating liquids at ambient conditions.

The primary objective of the current penetration tests was to obtain the distribution profiles for fuel oil hydrocarbons (represented by *n*-hexadecane) and water, along with effective diffusion coefficients and other sorption parameters. In this work, the results are primarily presented using a sorption coefficient, which is a measure of the rate of solvent uptake at times much less than that needed to achieve equilibrium saturation and an effective diffusion coefficient, which is a measure of the rate of change of solvent content as derived below in the ''Materials and Methods'' section. For readers unfamiliar with this terminology, we refer to a more detailed discussion in the article by Baglayeva and coauthors (Baglayeva et al. 2016). The use of short times was selected to assure incomplete pore filling of wood blocks, and thus allow the application of a continuous-source diffusion model at ambient temperature and pressure. The following flood-related wood contamination scenarios were considered:

1. *n*-Hexadecane sorption into wood at ambient temperature and humidity, which represents fuel oil spills without floods.

2. *n*-Hexadecane sorption into wood at ambient temperature and humidity followed by sorption of water, which represents a fuel oil tank rupture followed by rising of flood water.

3. Water sorption into wood at ambient temperature and humidity followed by *n*-hexadecane sorption, which represents the rising of flood water followed by a fuel oil tank rupture, or the draining of flood water with a layer of fuel oil (from flooded vehicles and storage tanks) on its surface after initial contact with the wood.

Southern yellow pine was used because of its common application as a wooden framing material with high strength, durability, and cost efficiency (Kaiser 1999). For mathematical simplicity, we have designed experiments that correspond to a one-dimensional diffusion model, with penetration along the longitudinal axis (derived using Fick's second law). The pertinent equations and limitations are detailed under ''Materials and Methods.''

Painting or coating of the wood member's lateral sides may also slow the process of air removal from wood tracheids, limiting the rate of liquid penetration. In an attempt to quantify this effect, the sides of some samples were coated with an epoxy resin to close lateral paths exposed by sample preparation. In this article, we use the data from short-time penetration to determine initial apparent diffusion coefficients and compare samples with and without lateral penetration paths. The entire penetration time profiles with accurate Fickian and empirical modeling involving multiple diffusion stages are considered in a separate publication (Baglayeva et al. 2016).

n-Hexadecane longitudinal profiling was obtained for all considered scenarios to elucidate the pathways of its penetration into wood. These results allowed us to investigate the interactions between the penetrating chemicals and contributed to an understanding of the dynamics of contaminant penetration into wood under disasters such as catastrophic floods.

Materials and Methods

Materials and reagents

Southern yellow pine (*Pinus taeda* or *palustris* or *echinata* or *elliottii*) with a specific gravity of 0.50 ± 0.03 g/cm³ and a moisture content of 7.4 ± 0.5 percent was used. The wood was cut into uniformly sized blocks of 3.8 by 3.9 cm² in cross-section and 15 cm in length. After preparation and before coating and use, wood blocks were stored for a brief period of time in a storage locker replicating the conditions of a summertime air-conditioned building (room temperature and 60% to 70% humidity), so the original water content was presumed to be maintained. In epoxy-coated samples, D.E.R. 331 Liquid Epoxy Resin (Dow Chemical Co., Midland, Michigan) with the addition of a curing agent was applied with a brush on all four transverse surfaces of the wood blocks, as recommended by the manufacturer. As a result of such coating, the potential surface effect (e.g., faster filling of the near-surface tracheids by penetrating liquids) was virtually eliminated.

n-Hexadecane (Alfa Aesar, Ward Hill, Massachusetts, 99%) and distilled water were used as model penetrating substrates. Chromatography-grade acetone, >99.5 percent and *n*-pentane, >99 percent (Fisher Scientific, Pittsburgh, Pennsylvania) were used as extraction solvents.

Mass uptake measurements

Short-term one-dimensional sorption of the two model liquids through uncoated and epoxy-coated wood blocks was measured according to the following eight scenarios:

1a. *n*-hexadecane sorption into uncoated wood,
1b. *n*-hexadecane sorption into epoxy-coated wood, i.e., same scenario as 1a but without lateral surface effects,
2a. *n*-hexadecane sorption into uncoated wood followed by water sorption,
2b. *n*-hexadecane sorption into epoxy-coated wood followed by water diffusion, i.e., same scenario as 2a but without lateral surface effects,
3a. water sorption into uncoated wood followed by *n*-hexadecane sorption,
3b. water sorption into epoxy-coated wood followed by *n*-hexadecane diffusion, i.e., same scenario as 3a but without lateral surface effects,
4a. water sorption into uncoated wood (used as a control sample),
4b. water sorption into epoxy-coated wood, i.e., same scenario as 4a but without lateral surface effects (used as a control sample).

The experiments were performed in an air-conditioned building at ambient pressure, a temperature of 22°C ± 2°C, and 50 to 60 percent relative humidity. Wood blocks were placed vertically in 200-mL glass beakers in a draft-free location along with the first liquid to be absorbed (*n*-hexadecane in Scenarios 1 and 2, and water in Scenarios 3 and 4). The liquid covered ca. 1 cm (maintained by refilling) of the bottom of the wood samples to ensure contact. The wood blocks were periodically taken out of the liquid, gently wiped with a lint-free tissue to remove sorbent droplets from the sample's surface, weighed, and then placed back into the beaker in such a way that any visible air bubbles were shaken off. An analytical balance Mettler H15 (Columbus, Ohio) with a weighing capacity of 160 g and a resolution of 0.5 mg was used.

The initial reading was conducted at 7 minutes, with subsequent measurements taken at regular intervals of 10 to 15 minutes depending on the penetration rate, as shown in Figure 1. The final reading was taken at 180 minutes. The length of the mass uptake experiments was chosen to assure the applicability of a continuous-source diffusion model, i.e., liquid sorption in a semi-infinite slab. At 180 minutes, the penetrating liquid reached ca. 2/3 height of the wood blocks (determined visually). Thus, the lateral front of absorbed liquid was still far from the end of wood block samples.

After the mass uptake measurements for the first penetrating liquid, the wood blocks were placed into similar 200-mL beakers containing the second liquid (water in Scenarios 2a and 2b, and *n*-hexadecane in Scenarios 3a and 3b). The gravimetric mass uptake measurements of the second liquid were performed similarly to the sorption analysis of the first liquid, as described above. All experiments were conducted at least in triplicate. The numerical values are reported in Table 1 as means ± standard deviations. Statistical outliers were identified by a standard *Q* test.

Analysis of *n*-hexadecane vertical distribution in wood samples

To estimate the distribution of absorbed *n*-hexadecane throughout a wood block (Scenarios 1 to 3), a two-step solid–liquid extraction was performed followed by gas chromatography–mass spectrometry analysis. This procedure has previously been shown to provide a quantitative recovery of *n*-hexadecane (Popova and Kozliak 2008). Immediately after the sorption experiments, the wood samples were cut into 1-cm-thick slices and further partitioned into smaller sectors, ca. 1 by 1 by 1 cm^3, to achieve a larger surface area. The resulting wood pieces (derived from each separate wood slice) were then placed in 22-mL vials with screw-top solid caps equipped with Teflon liners. After the first extraction solvent (acetone, 14.0 mL) was added into the vials, the cold-solvent extraction of *n*-hexadecane on a rotary shaker was carried out for 4 days (100 rpm, room temperature). Later the first extract was removed by decantation, and the second solvent (*n*-pentane, 14.0 mL) was added to the wood samples, followed by 4 days of extraction under the same conditions.

Aliquots of 10 μL were taken from each of the extracts, diluted 100 times in the solvent used for extraction (i.e., acetone or *n*-pentane), and analyzed using an Agilent 5890 Series II gas chromatograph with a 5972 mass spectrometry detector (Agilent Technologies, Santa Clara, California) equipped with an autosampler (7386B series) using 2-mL vials. The chromatographic separation was carried out on a DB-5MS+DG column (30 m by 0.25 mm by 0.25 μm column and 10-m Duraguard column) obtained from Agilent Technologies. A sample volume of 0.5 μL was injected in a 30:1 split ratio. Helium was used as a carrier gas at a constant flow rate of 1.0 mL/min. The oven temperature program started at 70°C for 1 minute followed by a ramp of 35°C/min to 300°C and then a hold of 3 minutes. The solvent delay was 2 minutes. The total run time was 10.6 minutes. Injector, detector, and transfer line temperatures were 250°C, 280°C, and 250°C, respectively. The electron ionization source and quadrupole analyzer temperatures were 350°C and 200°C, respectively. Mass spectrometry data were acquired in the scan mode in a mass range of *m/z* 40 to 600. External calibration was conducted with a series of *n*-hexadecane standard dilutions as detailed elsewhere (Popova and Kozliak 2008).

Evaluation of sorption parameters

Mass uptake values (*M*%) at different time periods were calculated as the difference between wood block weights W_t and $W_{t=0}$ at times t and $t_0 = 0$, respectively, over the initial weight of a wood block (Siau 1995):

$$M = \frac{W_t - W_{t=0}}{W_{t=0}} \qquad (1)$$

The sorption coefficients (a measure of the rate of solvent uptake at times much less than that needed to achieve equilibrium saturation) of *n*-hexadecane and water in wood (*S*; kg/m² s$^{1/2}$) were estimated as the slopes of the following linear plots:

$$\frac{(W_t - W_{t=0})}{A_c} = f(t^{1/2}) \qquad (2)$$

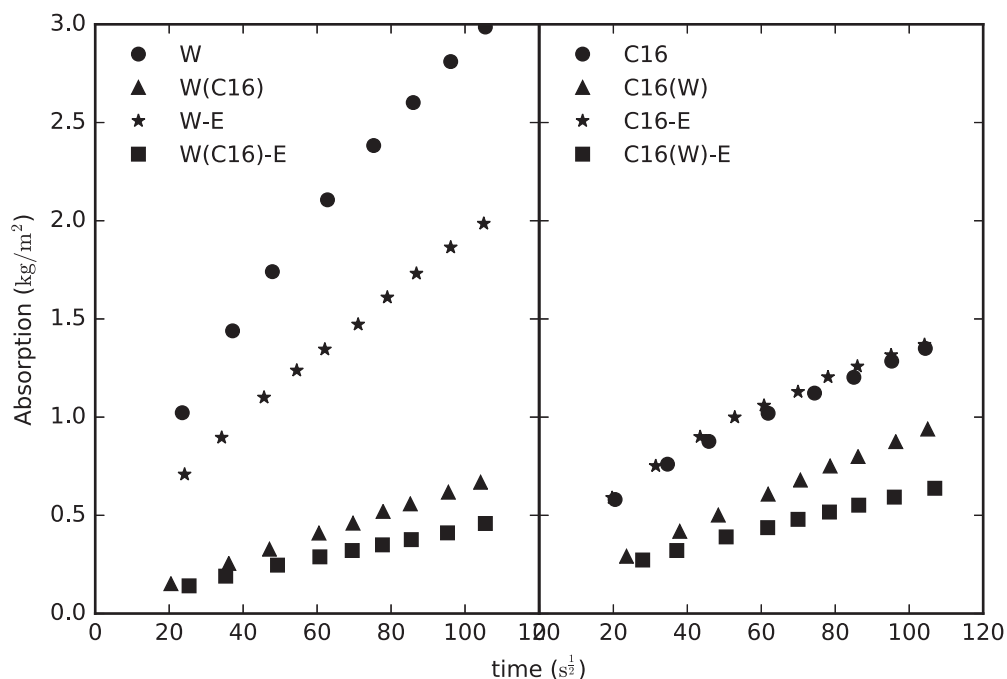where A_c is the surface area of the wood block in contact

Figure 1.—Short-term (180-min) sorption of water, W (left), and n-hexadecane, C16 (right), as a function of square root of immersion time for representative samples of uncoated and epoxy-coated wood under Scenarios 1 through 4. The legend denotes the solvent being absorbed, followed in parentheses by the previous solvent, if any. Epoxy coating is denoted with an E.

with the liquid in square meters:

$$A_c = hw + 2dh + 2dw \qquad (3)$$

where h (3.9 ± 0.1 cm) and w (3.8 ± 0.1 cm) are the height and the width of a wood block (''height'' actually means the width in the other direction), and d is the depth at which the wood block was immersed in the liquid (i.e., 1.0 ± 0.1 cm), measured in radial, tangential, and longitudinal directions, respectively. The nonzero y intercept of this plot was ignored (Baglayeva et al. 2016).

Table 1.—The end-point short-term (180-min) values of mass uptake and corresponding sorption and apparent diffusion coefficients for the one-dimensional sorption of water or n-hexadecane through uncoated and epoxy-coated wood blocks.[a]

Scenario	Penetrating liquid	Matrix	Mass uptake, M (%)[b]	Sorption coefficient, S ($\times 10^{-3}$ kg/m^2 s$^{1/2}$)[c]	Apparent end-grain diffusion coefficient, D_{app} ($\times 10^{-7}$ m^2/s)[d]	Apparent lateral diffusion coefficient, D^S_{app} ($\times 10^{-7}$ m^2/s)[e]
1a	n-Hexadecane	Uncoated wood	5.8 ± 0.3	10.1 ± 1.7	2.8 ± 0.1	2.8 ± 1.1
1b	n-Hexadecane	Epoxy-coated wood	5.0 ± 0.1	9.0 ± 0.5	2.9 ± 0.1	NA[f]
3a	n-Hexadecane	Uncoated wood partially saturated with water	3.0 ± 0.2	7.9 ± 0.8	3.3 ± 0.1	2.6 ± 0.4
3b	n-Hexadecane	Epoxy-coated wood partially saturated with water	2.3 ± 0.1	4.6 ± 0.4	2.9 ± 0.1	NA
4a	Water	Uncoated wood	10.3 ± 0.4	23.7 ± 0.7	3.1 ± 0.1	2.6 ± 0.7
4b	Water	Epoxy-coated wood	7.7 ± 1.1	15.7 ± 2.3	3.2 ± 0.1	NA
2a	Water	Uncoated wood partially saturated with n-hexadecane	2.7 ± 0.2	6.2 ± 0.6	3.5 ± 0.1	NA
2b	Water	Epoxy-coated wood partially saturated with n-hexadecane	1.6 ± 0.2	3.8 ± 0.5	3.2 ± 0.1	NA

[a] Values are means of triplicate samples ± standard deviations.
[b] Mass uptake values were calculated by using Equation 1.
[c] Sorption coefficients were estimated by Equation 2.
[d] End-grain apparent diffusion coefficients were calculated using Equation 7.
[e] Apparent lateral diffusion coefficients were calculated using Equation 9.
[f] NA = not applicable, as it was not feasible to observe the lateral front of penetrating liquid either because of the epoxy coating or presaturation of wood blocks with the first penetrating liquid.

For our calculations, we used $A = A_c$ as the contact area for both coated and uncoated blocks. One might argue that the epoxy-coated blocks should have a diffusion area equal to the cross-sectional area, hw. However, given the dominance of end-grain longitudinal sorption over lateral sorption, the actual value of A should be somewhere between hw and A_c. To eliminate this uncertainty and to assure consistency with the prior literature, the same area, $A = A_c$, was used throughout this work.

Evaluation of apparent diffusion coefficients

Non–steady-state one-dimensional diffusion can be described by Fick's second law if the initial region of a penetrating liquid's sorption curve remains linear up to at least 60 percent of the total mass uptake, regardless of the material thickness (Chin et al. 1999):

$$\frac{\partial C}{\partial t} = -D \frac{\partial C}{\partial x^2} \quad (4)$$

For one-dimensional diffusion through a planar sheet of length L subject to the boundary conditions, where C is concentration, x is the position along the length of the sample, and t is the time from start of diffusion, and the boundary conditions are

at $x = 0$, $C = C_1$, $t \geq 0$;

at $x = L$, $C = 0$, $t \geq 0$, approximating a semi-infinite slab for suitably short terminal time period, $t_{end} \approx t_\infty$; and

$C = C_0$ for $0 \leq x \leq L$ at $t = 0$

i.e., the entire sheet is initially at a uniform concentration of C_0 throughout at time $t = 0$. Then, if W_t denotes the total mass of diffusing substance that has entered the domain at time t and W_∞ reflects the corresponding quantity after an infinite time period, the solution of Equation 4 is as follows (Crank 1975):

$$\left(\frac{W_t - W_{t=0}}{W_{t=\infty} - W_{t=0}} \right) = \left(1 - \frac{8}{\pi} \sum_{n=0}^{\infty} \frac{1}{(2n+1)^2} e^{-D(2n+1)^2 \pi^2 t / L^2} \right) \quad (5)$$

For the initial region of a liquid's sorption at short times, Equation 5 can be further simplified by truncating to the first term of the series expansion of the exponential term, resulting in Equation 6 (Siau 1995):

$$\frac{W_t - W_{t=0}}{W_{t=\infty} - W_{t=0}} = \left(\frac{4}{L\sqrt{\pi}} \right) \sqrt{Dt} \quad (6)$$

where L is the diffusion distance perpendicular to a planar sheet and D is the effective diffusion coefficient (a measure of the rate of change of solvent uptake specific to the solvent-material pair) in square meters per second.

For rectangular-shaped wood blocks with diffusion from one end (i.e., being half of that for immersed samples), Equation 6 can be rewritten as

$$\frac{W_t - W_{t=0}}{W_{t=\infty} - W_{t=0}} = \frac{2}{\sqrt{\pi}} \left(\frac{A}{V} \right) \sqrt{Dt} \quad (7)$$

where A is the cross-sectional area of a wood block perpendicular to the movement of the liquid in square

meters and V is the total volume of a wood block in cubic meters:

$$V = hwl \quad (8)$$

with h, w, and l being the height, width, and length of a wood block, respectively.

To determine the mass uptake equilibrium values for n-hexadecane and water sorption in uncoated and epoxy-coated wood, wood samples were fully submerged into the given liquid. For the scenarios with uncoated wood, similar experiments were repeated using chip-size (3 by 15 by 15 mm^3) wood samples to accelerate the achievement of mass uptake equilibrium; the values matched.

Equation 7 was used to calculate the short-term end-grain (i.e., total longitudinal) apparent diffusion coefficient (D_{app}), observed for the initial penetration (i.e., $\leq 10\%$ of the total mass uptake) of n-hexadecane and water. This approach, though qualitatively accurate, has the following quantitative limitations. Our experimental configuration deviates slightly from the one-dimensional case as the end of the sample is immersed to a small but finite depth. At long diffusion times, the lateral area is small relative to the total sample length, but at short times, as considered in this article, the open tracheids on the lateral faces may cause the initial uptake rate to be influenced by the penetration through the lateral faces. Because the obtained numerical values are discussed as merely effective parameters, the model used may be deemed adequate.

The lateral (i.e., surface longitudinal) apparent diffusivities (D^S_{app}) were estimated by Equation 9:

$$D^S_{app} = \frac{z^2}{4t} \quad (9)$$

where z, measured in meters (for any value reported in Table 1) or centimeters, is the length of the chemical's lateral penetration front. The value of z was determined visually as a mean value of the apparent liquid front heights on all four sides of the wood blocks. To enable its accurate determination, a grid with a resolution of 0.2 cm was manually sketched on all four sides of the wood blocks using a graphite pencil.

Results and Discussion

Mass uptake values and apparent sorption coefficients

Figure 1 illustrates the initial penetration (below 10% of the total mass uptake; Table 1) of n-hexadecane and water into wood blocks under different scenarios. The slopes observed for all experimental scenarios were nearly constant throughout the allotted time range (Fig. 1), allowing for estimation of sorption coefficients and apparent short-term diffusivities using Fick's second law (Table 1).

In uncoated wood samples, the measured sorption coefficients and mass uptake values were influenced by the nature of the penetrating liquid and resulting contaminant–matrix interactions. Water, as a polar wood-swelling contaminant, absorbs both more efficiently and faster than hydrophobic n-hexadecane (M and S, respectively; Table 1). The application of epoxy coating slowed penetration of water and reduced the extent of wood swelling (as observed visually). The most plausible explanation of this effect is blocking the path for air bubbles to leave the lumina in

coated wood. In addition, because the epoxy resin is hydrophobic, the water sorption is limited to the untreated wood tracheids, reducing the total water uptake and thus wood swelling (Frihart 2006). By contrast, the mass uptake and sorption rate values of nonpolar *n*-hexadecane as a single penetrating liquid (Scenario 1) were less dependent on whether an epoxy coating was applied to the external faces of the wood block (Scenarios 1a and 1b), with comparable values for each condition (*M* and *S*, respectively; Table 1). Air bubbles may be more readily dissolved in nonpolar *n*-hexadecane than in water (Baglayeva et al. 2016).

When the wood was first contaminated with *n*-hexadecane (Scenario 2), the subsequent penetration of water was reduced more than threefold (*M*; Table 1). Apparently, sorption of water within polar tracheids involves significant interactions with their surface, e.g., via hydrogen bonding with cellulosic materials (Mackay and Gschwend 2000). As a result of the prior saturation of wood capillaries with *n*-hexadecane, these polar sites become inaccessible, thus reducing the water sorption rate (*S*; Table 1).

These results may be compared with the previously reported reduction in water sorption rates for hydrophobically modified, e.g., acetylated wood (Popescu et al. 2014, Himmel and Mai 2015). Both processes may involve similar mechanisms, such as the bulking of the cell wall. Corroborating this suggestion, presaturation of acetylated wood with wax, a substance with a hydrophobicity similar to hydrocarbons, further decreased the rate of water sorption (Scholz et al. 2012).

By contrast, when the order of the penetrating liquids was switched (Scenario 3), presaturation of uncoated wood with water only slightly reduced the subsequent *n*-hexadecane mass uptake (*M*; Table 1). If water and *n*-hexadecane use different paths for their penetration into wood, i.e., tracheids and hydrophobic cell wall fractions, respectively, this observation would be expected. However, even if the main longitudinal path of *n*-hexadecane penetration is still via the large tracheids, just as for water, the lower density of *n*-hexadecane than that of water would enable its vertical passage through the aqueous layer toward the top of the liquid penetration zone. In addition, when the cellulosic portion of wood absorbs water, the integrity of wood cell walls may be compromised by opening otherwise blocked tracheids, thus producing additional diffusion paths across the fibers. The combination of these two effects may explain the high subsequent *n*-hexadecane sorption rate (*S*; Table 1).

Covering wood sample lateral surfaces with epoxy further lowered the sorption coefficients and mass uptake values for the second of two penetrating liquids (Scenarios 2b and 3b compared with 2a and 3a, respectively). This observation contrasts with the apparent lack of effect of coating the wood sample lateral surface on the rate of *n*-hexadecane absorption as a single liquid. Coating appears to only be a factor when water is absorbed. Furthermore, the order of the penetrating liquids did not make a significant difference (Scenarios 2b and 3b), resulting in similar *M* and *S* values for *n*-hexadecane and water in epoxy-coated presaturated wood (*S* and *M*, respectively; Table 1). These observations confirmed our hypotheses that trapped air bubbles as a result of wood coating may be dissolved in hydrocarbons and that wood swelling as a result of water absorption could be the other significant factor in whether wood coating affects liquid penetration.

However, the observation that the presaturation of a wood block with one contaminant did not prevent the subsequent sorption of another but merely slowed it may suggest that these two liquids use different penetration paths owing to their differences in polarity. This hypothesis will be confirmed in subsequent sections.

End-grain and lateral surface apparent diffusion coefficients

The numerical values of both apparent diffusivities (D_{app}) and apparent lateral diffusivities (D^{S}_{app}), determined by Equations 7 and 9, respectively, are listed in Table 1. It is of note that parameters *S* (discussed in the previous section) and *D,* despite their apparent similarity, reflect different aspects of the sorption process. Whereas *S* describes both the sorption speed and capacity, *D* is a measure of just the sorption speed. Thus, the additional sorption capacity available for water as a wood-swelling chemical was not expected to alter *D* but was expected to be influenced by molecular parameters affecting the value of *S*.

Indeed, water and *n*-hexadecane as single penetrating liquids had similar apparent diffusivities (D_{app}) into ambient wood (Scenarios 4 and 1; Table 1), regardless of their polarity and lateral effects (i.e., penetration into either uncoated or epoxy-coated wood). This observation indicates that the initial penetration of liquids into wood may be owing to a simple end-grain sorption into tracheids and is not affected by the affinity of sorbed molecules to the wood matrix. The apparent diffusivities into presaturated wood also turned out to be similar, corroborating the hypothesis of different, mutually independent paths for water and *n*-hexadecane penetration (Scenarios 2 and 3, D_{app}; Table 1).

The determination of apparent lateral diffusivities (D^{S}_{app}) by a different, nongravimetric method (Eq. 9) helped to further elucidate the wood absorption pathways. This determination was limited to the cases listed in Table 1 because the visual monitoring of the liquid penetration front in epoxy-coated and presaturated wood blocks was not feasible. The D^{S}_{app} values calculated by this method matched the corresponding end-grain apparent diffusivities (Table 1), thus mutually validating both methods of determining apparent diffusivities. The observed similarity of apparent end-grain and lateral diffusivities between water and *n*-hexadecane as single penetrating liquids also indicated that there is no preference for the liquid's sorption near the lateral sides in terms of the penetration speed.

Longitudinal distribution of *n*-hexadecane within the wood blocks

The longitudinal distributions of *n*-hexadecane in both uncoated and epoxy-coated wood samples under various scenarios are shown in Figure 2 as fractions of the total introduced *n*-hexadecane in sequential wood slices, as determined using chromatography.

Even though the trends in *n*-hexadecane (as a single penetrating liquid) sorption parameters in uncoated and epoxy-coated wood were similar (Table 1), there was a significant difference in penetration profiles (Fig. 2). Namely, in the epoxy-treated wood samples (Figs. 2d through 2f), most of the absorbed *n*-hexadecane concentrated near the base of the block, whereas in the case of
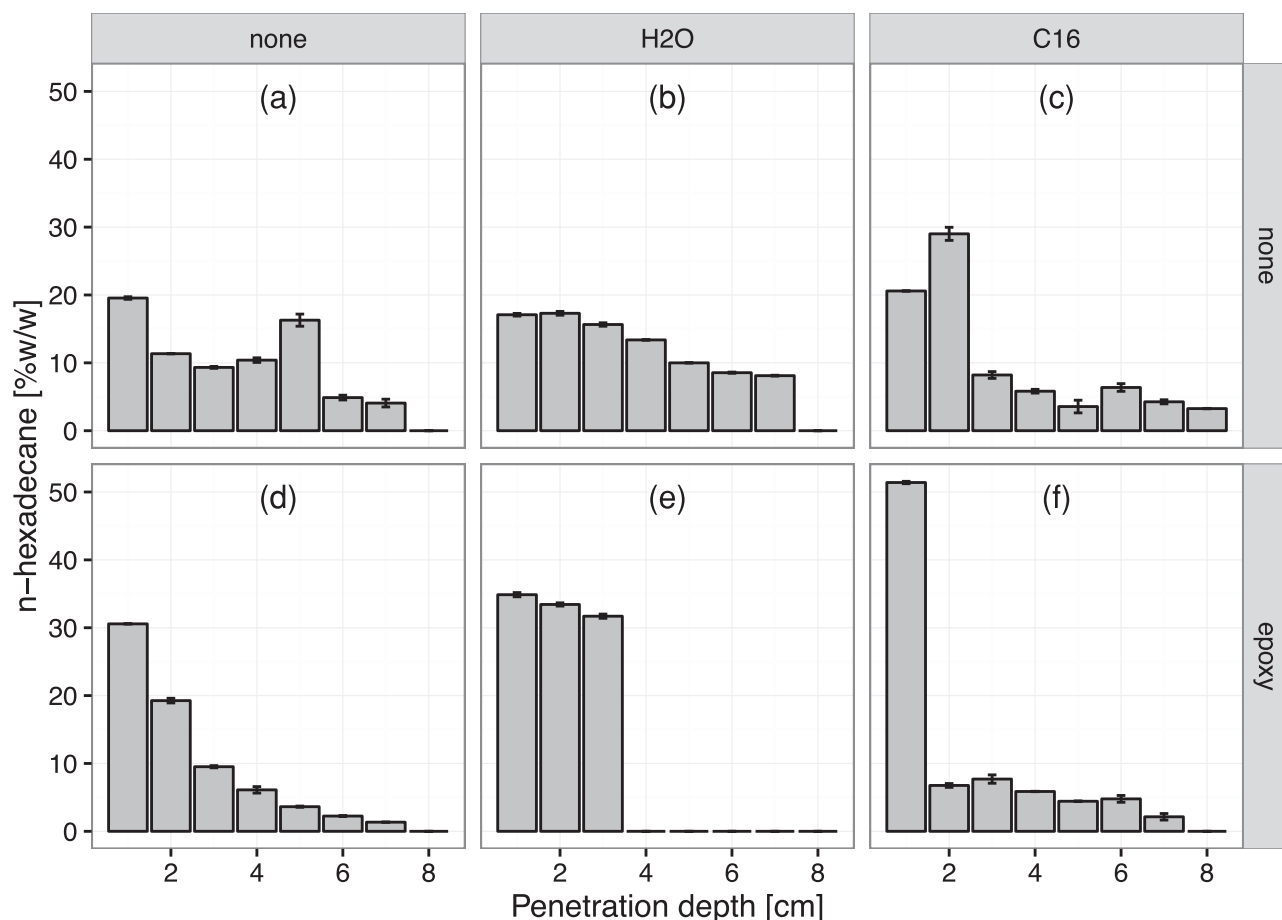
Figure 2.—Distribution of n-hexadecane in wood blocks after 180 minutes of contamination expressed as n-hexadecane amount (percent by weight) versus n-hexadecane penetration depth (centimeters) under various flood scenarios. Panels a through c represent uncoated wood, panels d through f represent epoxy-coated blocks. Samples in a and d were immersed in n-hexadecane only, samples in b and e were immersed in water before immersion in n-hexadecane, and samples in c and f were immersed in n-hexadecane before immersion in water. The error bars represent standard errors for triplicate samples.

uncoated wood, *n*-hexadecane was distributed almost uniformly throughout the entire wood sample (Figs. 2a through 2c). Because the liquid penetration depth is governed strictly by capillary forces under no external pressure (Smith and Purslow 1960, Morgan and Purslow 1973), the observed difference is most likely owing to the lower accessibility of the capillary path. This, in turn, may be caused by the resistance to movement caused by the air entrained inside the tracheids, which would be more pronounced in epoxy-coated wood samples. Even though the air bubbles may eventually dissolve in *n*-hexadecane, their temporary presence may redirect the flow away from the longitudinal capillaries. The bulk rate of hydrocarbon penetration may remain unaltered but its direction may be shifted to smaller voids near the end-grain surface.

n-Hexadecane longitudinal penetration profiles observed in water-saturated wood samples were rather similar to those of pure hydrocarbon uptake (Figs. 2b and 2a, respectively). Greater mass uptake values in uncoated wood blocks resulted in a more uniform distribution of *n*-hexadecane within the wood blocks, whereas in the similar epoxy-coated wood samples virtually all *n*-hexadecane concentrated within the first 3 cm from the base of the wood block (Figs. 2b and 2e, respectively). These results

confirm the above proposed hypothesis that (1) lower density of *n*-hexadecane (than that of water) caused its penetration through large water-saturated tracheids and (2) epoxy coating in the presence of water significantly limits *n*-hexadecane penetration into the upper layers of wood blocks. Perhaps when the alternate lateral paths of water penetration through smaller capillaries are not accessible because of coating, the *n*-hexadecane upward movement based on the difference in density is hindered, as confined excess water cannot readily "yield" its way to the hydrocarbon.

When followed by water, *n*-hexadecane distribution profiles in uncoated and epoxy-coated wood were similar, with ca. 70 percent of the hydrocarbon concentrated near the base of the wood blocks (Figs. 2c and 2f). This observation was in sharp contrast to the reverse order of liquid penetration when the presaturation of wood with water did not create much of the barrier to subsequent *n*-hexadecane absorption, with its significant penetration toward the top of the wood block (Fig. 2b). Comparison of these penetration profiles with those obtained for the scenarios when *n*-hexadecane was applied as a single liquid (Figs. 2a and 2d) confirms a significant effect of water as the second penetrating liquid on the *n*-hexadecane redistribution within the wood sample.

This unexpected effect of water forcing *n*-hexadecane repositioning back to the base of the wood block provides further evidence that these two immiscible liquids use different (although overlapping) penetration paths due to the differences in their physical properties and resulting interactions with wood. Water causes wood swelling by penetration through the cell walls and is also attracted by polar functional groups within the cellulosic structure of the wood. In contrast, *n*-hexadecane lacks these capabilities and thus its absorption in wood strongly depends on tracheid size and availability, the occurrence of an interconnecting pit system, and the presence of natural barriers such as air and various deposits (e.g., gums and resins; Stone and Forderrenther 1956, Forest Products Laboratory 1999). Even though tracheids represent a preferred route for water, this wood-swelling liquid can use alternate paths when the primary path is blocked. Adsorption-assisted penetration would be most significant in narrow capillaries, whereas swelling would create new channels. Water rising through these alternate channels may then enter the *n*-hexadecane–filled tracheids above the hydrocarbon layer, creating a driving force for *n*-hexadecane to move back toward the base of the wood. This effect is facilitated by gravity and by the repulsion of this nonpolar liquid by the cellulose walls of the tracheids.

Implications for different scenarios of catastrophic floods

With respect to catastrophic floods, if the wood is presaturated with water, semivolatile nonpolar hydrocarbons, such as those in fuel oil, will still penetrate into the wood in similar amounts, apparently through different paths.

In contrast, if the wood is first contaminated with fuel oil, e.g., as a layer on top of rising water, the subsequent penetration of water may actually decrease the severity of the contamination by inducing the hydrocarbons to concentrate near the exterior surface. Because the hydrocarbons are near the exterior surface, remediation should be fairly straightforward, using techniques such as those developed by Kozliak and Beklemishev (2006) and Kozliak and Seames (2010, 2011).

It should be noted that wood swelling resulting from the subsequent exposure of the wood to water after hydrocarbon penetration also tends to seal off the accessible tracheids. This effect was most conspicuous with the epoxy-coated wood. Therefore, it may still be more difficult to decontaminate wood under these conditions compared with wood that absorbed just the hydrocarbons.

Conclusions

Presaturation of wood blocks with water only slightly decreased the subsequent sorption of *n*-hexadecane. Conversely, the prior contamination of wood blocks with *n*-hexadecane significantly reduced the subsequent penetration of water. However, the *n*-hexadecane distribution in this second scenario was affected by subsequent water sorption, resulting in counterintuitive hydrocarbon relocation back toward the wood block's base. Coating of wood block lateral surfaces with epoxy only reduced the liquid's mass uptake in scenarios involving water, perhaps because of persistent air bubbles (less soluble in water than in hydrocarbons) and restrictions imposed on wood swelling by the coating. Similar obtained values of apparent end-

grain and lateral diffusion coefficients in uncoated and epoxy-coated wood indicate that lateral paths are not preferential. The results also suggest that water and *n*-hexadecane use different (although overlapping) penetration paths owing to the differences in their physical properties.

Literature Cited

Baglayeva, G., G. Krishnamoorthy, C. R. Frihart, W. S. Seames, J. O'Dell, and E. I. Kozliak. 2016. Modeling of *n*-hexadecane and water sorption in wood. *Forest Prod. J.* 67(7/8):401–412.

Barrera-García, V. D., R. D. Gougeon, T. Karbowiak, A. Voilley, and D. Chassagne. 2008. Role of wood macromolecules on selective sorption of phenolic compounds by wood. *J. Agric. Food Chem.* 56(18):8498–8506.

Chin, J. W., T. Nguyen, and K. Aouadi. 1999. Sorption and diffusion of water, salt water, and concrete pore solution in composite matrices. *J. Appl. Polym. Sci.* 71(3):483–492.

Comstock, G. L. 1970. Directional permeability of softwoods. *Wood Fiber Sci.* 1(4):283–289.

Crank, J. 1975. The Mathematics of Diffusion. Clarendon Press, Oxford, UK. 414 pp.

Forest Products Laboratory. 1999. Wood handbook—Wood as an engineering material. General Technical Report FPL-GTR-113. Forest Products Laboratory, Madison, Wisconsin. 463 pp.

Frihart, C. R. 2006. Are epoxy–wood bonds durable enough? *In:* Wood Adhesives 2005: Discussion Forum. Forest Products Society, San Diego, California.

Himmel, S. and C. Mai. 2015. Effects of acetylation and formalization on the dynamic water vapor sorption behavior of wood. *Holzforschung* 69(5):633–643.

Kaiser, J.-A. 1999. Southern yellow pine: A long-time favorite. *Wood Prod.* 104(10):33–34.

Khazaei, J. 2008. Water absorption characteristics of three wood varieties. *Cercet. Agron. Moldova* XLI(2[134]):5–16.

Koponen, S. 1999. Effect of wood cell structure on diffusion properties—Sorption tests. *Helsinki Univ. Technol. LSEBP Publ.* 103:35–36.

Kozliak, E. I. and M. K. Beklemishev. 2006. Removal of toxic/hazardous chemicals absorbed in building materials. US patent 7,144,725. Issued December 5, 2006.

Kozliak, E. I. and W. S. Seames. 2010. Photocatalyst-induced reduction of semivolatile organic chemicals. US patent 7781638. Issued August 24, 2010.

Kozliak, E. I. and W. S. Seames. 2011. Absorbent mediated reduction of organic chemicals from solid building materials. US patent 8,012,242. Issued September 6, 2011.

Krabbenhoft, K. and L. Damkilde. 2004. A model for non-Fickian moisture transfer in wood. *Mater. Struct.* 37(273):615–622.

Kumaran, M. K. 1999. Moisture diffusivity of building materials from water absorption measurements. *J. Therm. Envelope Build. Sci.* 22:349–355.

Mackay, A. A. and P. M. Gschwend. 2000. Sorption of monoaromatic hydrocarbons to wood. *Environ. Sci. Technol.* 34(5):839–845.

Malkov, S., V. Kuzmin, V. Baltakhinov, and P. Tikka. 2003. Modelling the process of water penetration into softwood chips. *J. Pulp Pap. Sci.* 29(4):137–143.

Malkov, S., P. Tikka, and J. Gullichsen. 2001. Towards complete impregnation of wood chips with aqueous solutions. Part 2: Studies on water penetration into wood chips. *Pap. Timber* 83(6):468–473.

Marcovich, N. E., M. M. Reboredo, and M. I. Aranguren. 1999. Moisture diffusion in polyester–woodflour composites. *Polymer* 40(26):7313–7320.

Morgan, J. W. W. and D. F. Purslow. 1973. Physical and chemical

aspects of preservative treatment by nonpressure methods. *Holzforschung* 27(5):153–159.

Petty, J. A. 1975. Relation between immersion time and absorption of petroleum distillate in a vacuum-pressure process. *Holzforschung* 29(4):113–118.

Petty, J. A. 1978a. Effects of solvent-exchange drying and filtration on the absorption of petroleum distillate by spruce wood. *Holzforschung* 32(2):52–55.

Petty, J. A. 1978b. Influence of viscosity and pressure on the radial absorption of non-swelling liquids by pine sapwood. *Holzforschung* 32(4):134–137.

Popescu, C.-M., C. A. S. Hill, S. Curling, G. Ormondroyd, and Y. Xie. 2014. The water vapour sorption behaviour of acetylated birch wood: How acetylation affects the sorption isotherm and accessible hydroxyl content. *J. Mater. Sci*. 49(5):2362–2371.

Popova, I. E. and E. I. Kozliak. 2008. Efficient extraction of fuel oil hydrocarbons from wood. *Sep. Sci. Technol*. 43(4):778–793.

Possani, L. F. K., R. L. Simoes, P. B. Staudt, and R. de P. Soares. 2014. Mutual solubilities of hydrocarbon–water systems with F-SAC. *Fluid Phase Equilib*. 384:122–133.

Scholz, G., A. Krause, and H. Militz. 2012. Full impregnation of modified wood with wax. *Eur. J. Wood Wood Prod*. 70(1–3):91–98.

Siau, J. F. 1995. Wood: Influence of Moisture on Physical Properties. Wood Science and Forest Products, Virginia Tech, Blacksburg. 227 pp.

Smith, D. N. and D. F. Purslow. 1960. Preservative treatment of pine sapwood. *Timber Technol*. 68:67–71.

Stone, J. E. and C. Forderrenther. 1956. Studies of penetration and diffusion into wood. *TAPPI* 39(10):679–683.